

Kinetic Geodesic Voronoi Diagrams in a Simple Polygon

Matias Korman* André van Renssen† Marcel Roeloffzen‡ Frank Staals§

Abstract

We study the geodesic Voronoi diagram of a set S of n linearly moving sites inside a static simple polygon P with m vertices. We identify all events where the structure of the Voronoi diagram changes, bound the number of such events, and then develop a kinetic data structure (KDS) that maintains the geodesic Voronoi diagram as the sites move. To this end, we first analyze how often a single bisector, defined by two sites, or a single Voronoi center, defined by three sites, can change. For both these structures we prove that the number of such changes is at most $O(m^3)$, and that this is tight in the worst case. Moreover, we develop compact, responsive, local, and efficient kinetic data structures for both structures. Our data structures use linear space and process a worst-case optimal number of events. Our bisector KDS handles each event in $O(\log m)$ time, and our Voronoi center handles each event in $O(\log^2 m)$ time. Both structures can be extended to efficiently support updating the movement of the sites as well. Using these data structures as building blocks we obtain a compact KDS for maintaining the full geodesic Voronoi diagram.

*Department of Computer Science, Tufts University, Medford, MA, USA, matias.korman@tufts.edu

†School of Computer Science, University of Sydney, Sydney, Australia andre.vanrenssen@sydney.edu.au

‡Dept. of Mathematics and Computer Science, TU Eindhoven, Eindhoven, The Netherlands
m.j.m.roeloffzen@tue.nl

§Dept. of Information and Computing Sciences, Utrecht University, Utrecht, The Netherlands f.staals@uu.nl

1 Introduction

Polygons are one of the most fundamental objects in computational geometry. As such, they have been used for many different purposes in different contexts. Within the path planning community, polygons are often used to model different regions. A simple example is when we have a robot moving within a building: in such a case we model all possible locations that a robot can reach by a polygon (the walls or any obstacle in the way form the boundary of this polygon). Then, the goal is to find a path that connects the source point and the destination and that minimizes some objective function. There are countless many results that depend on the exact function used (distance traveled [10], time needed to reach [17], number of required turns [27], etc.) Paths that minimize distance are often called *geodesics*.

Two of the most fundamental problems in this setting are constructing *shortest path maps* and *augmented Voronoi diagrams*. A shortest path map (or SPM for short) is a partition of the space into regions so that points in the same region travel in the same way to the fixed source [10, 13]. The exact definition of “in the same way” depends on the exact problem setting, but it often means that paths are *combinatorially* the same, that is, they have the same internal vertices. Augmented Voronoi diagrams are a generalization of SPMs for the case in which we have more than one fixed source and we are interested in the topology of the path to the closest source [4]. See Fig. 1 for an illustration. These structures are of critical importance in obtaining efficient solutions to related problems such as finding center points, closest pairs, nearest neighbors, and constructing spanners [22, 23].

It often happens that while we are moving to our destination, that destination is also moving. For example, when two agents try to meet, one wants to evade the other, or one simply needs to meet up with a second one that is doing a different task [16]. Since it is very costly to recompute the solution after each infinitesimal movement, the aim is to somehow maintain some information from which we can easily obtain the solution, and update this information only when the solution has significant changes. A data structure that can handle such a setting is known as a *kinetic data structure* (or KDS for short) [6]. There is a wide range of problems that have been studied in this setting. We refer to the survey by Basch et al. [6] for an overview of these results.

Surprisingly, there is very little work that combines all three of the above concepts (polygons, shortest paths, and kinetic data structures). We are aware of only two results. Aronov et al. [3] present a KDS for maintaining the shortest path map of a single point moving inside a simple polygon, and Karavelas and Guibas [14] give a KDS to maintain a *constrained Delaunay triangulation* of a set of moving points. This allows them to maintain nearest neighbors and the geodesic hull.

We present the first KDS to maintain the full (augmented) geodesic Voronoi diagram of a set of point sites moving inside a simple polygon, thus generalizing the above results. We carefully analyze when and how often it can change. To this end, we prove tight bounds on the number of combinatorial changes in a single bisector, and on the trajectory of a Voronoi center. Our results provide an important tool for maintaining related structures in which the agents (sites) move linearly within the simple polygon (e.g. minimum spanning trees, nearest-neighbors, closest pairs, etc.).

Related Work. Our data structures are based on the Kinetic Data Structures (KDS) framework introduced by Basch et al. [6]. In this framework motions are assumed to be known in advance. Each KDS maintains a set of *certificates* that together certify that the KDS currently correctly

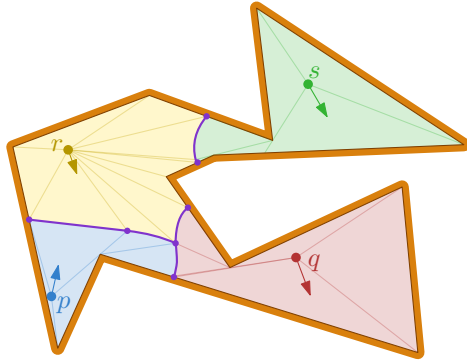


Fig. 1: The (augmented) geodesic Voronoi diagram of four moving sites p , q , r , and s .

represents the target structure. Typically these certificates involve a few objects each and represent some simple geometric primitive. For example a certificate may indicate that three points form a clockwise oriented triangle. As the points move these certificates may become invalid, requiring the KDS to update. This requires repairing the target structure and creating new certificates. Such a certificate failure is called an (*internal*) *event*. An event is *external* if the target structure also changes. The performance of a KDS is measured according to four measures. A KDS is considered *compact* if it requires little space, generally close to linear, *responsive* if each event is processed quickly, generally polylogarithmic time, *local* if each site participates in few events, and *efficient* if the ratio between external and internal events is small, generally polylogarithmic. Note that for efficiency it is common to compare the worst-case number of events for either case.

Let S be a set of n point sites moving linearly in a space P , that is, each point moves with a fixed speed and direction. The *Voronoi diagram* $\text{VD}_P(S)$ of S is a partition of P into n regions, one per site $s \in S$, such that for any point q in such a region \mathcal{V}_s is closer to s than to any other site from S . Guibas et al. [11] studied maintaining the Voronoi diagram in case $P = \mathbb{R}^2$ and distance is measured by the Euclidean distance. They prove that $\text{VD}_{\mathbb{R}^2}(S)$ may change $\Omega(n^2)$ times, and present an a KDS that handles at most $O(n^3\beta_4(n))$ events, each in $O(\log n)$ time. Here, $\beta_z(n) = \lambda_z(n)/n$ and $\lambda_z(n)$ is the maximum length of a Davenport-Schinzel sequence of n symbols of order z [25]. Their results actually extend to slightly more general types of movement. It is one of the long outstanding open problems if this bound can be improved [8, 9]. Only recently, Rubin [24] showed that if all sites move linearly and with the same speed, the number of changes is at most $O(n^{2+\varepsilon})$ for some arbitrarily small $\varepsilon > 0$. For arbitrary speeds, the best known bound is still $O(n^3\beta_4(n))$. When the distance function is specified by a convex k -gon the number of changes is $O(k^4n^2\beta_z(n))$ [2]. Here, and throughout the rest of the paper z denotes some small constant.

Let P be a simple polygon with m vertices, and let $\pi(s, q)$ be the shortest path between s and q that stays entirely inside P . We measure length of a path by the sum of the Euclidean edge lengths. Such a shortest path is known as a geodesic, and its length as the *geodesic distance*. With some abuse of notation we use $\pi(s, q)$ to denote both the shortest path between s and q and its length.

Aronov was the first to study the geodesic Voronoi diagram [4]. He proved that when the sites in S are static, $\text{VD}_P(S)$ has complexity $O(n + m)$. The same bound applies for the augmented geodesic Voronoi diagram. Moreover, he presented an $O((n + m) \log(n + m) \log n)$ time algorithm for constructing $\text{VD}_P(S)$, which was improved to $O((n + m) \log(n + m))$ by Papadopoulou and Lee [23]. Recently, there have been several improved algorithms [15, 20] which ultimately lead to an optimal $O(m + n \log n)$ time algorithm by Oh [19]. Furthermore, Agarwal et al. [1] recently showed that finding the site in S closest to an arbitrary query point $q \in P$ — a key application of geodesic Voronoi diagrams — can be achieved efficiently even if sites may be added to, or removed from, S .

There are no known results on maintaining an (augmented) geodesic Voronoi diagram when multiple sites S move continuously in a simple polygon P . In case there is only one site s , Aronov et al. [3] presented a KDS that maintains the shortest path map SPM_s of s . Their data structure uses $O(m)$ space, and processes a total of $O(m)$ events in $O(\log m)$ time each¹. Karavelas and Guibas [14], provide a KDS to maintain a constrained Delaunay triangulation of S . This allows them to maintain the geodesic hull of S w.r.t. P , and the set of nearest neighbors in S (even in case P has holes). Their KDS processes $O((m + n)^3\beta_z(n + m))$ events in $O(\log(n + m))$ time each.

Organization and Results. We present a kinetic data structure to maintain the geodesic Voronoi diagram $\text{VD}_P(S)$ of a set S of n sites moving linearly inside a simple polygon P with m vertices. To

¹ The original description by Aronov et al. [3] uses a dynamic convex hull data structure that supports $O(\log^2 m)$ time queries and updates. Instead, we can use the data structure by Brodal and Jacob [7] which supports these operations in $O(\log m)$ time.

Event	Lower bound	Upper bound
1, 2-collapse/expand	$\Omega(m^2n)$	$O(m^2n^2)$
1, 3-collapse/expand	$\Omega(mn \min\{n, m\})$	$O(m^2n^2 \min\{m\beta_z(n), n\})$
2, 2-collapse/expand	$\Omega(m^3n)$	$O(m^3n\beta_4(n))$
2, 3-collapse/expand	$\Omega(mn^2 + m^3n)$	$O(m^3n^2\beta_4(n)\beta_z(n))$
3, 3-collapse/expand	$\Omega(mn^2 + m^2n)$	$O(m^3n^3\beta_z(n))$
vertex	$\Omega(m^2n)$	$O(m^2n\beta_4(n))$

Tab. 1: The different types of events at which the geodesic Voronoi diagram changes, and their number. At an a, b -collapse event two vertices of $\text{VD}_P(S)$ with degrees a and b collide and one disappears. Similarly, at an a, b -expand one such a vertex appears. At a vertex event a vertex of $\text{VD}_P(S)$ collides with a vertex of P .

this end, we prove a tight $O(m^3)$ bound on the number of combinatorial changes in a single bisector, and develop a compact, efficient, and responsive KDS to maintain it (Section 3). Our KDS for the bisector uses $O(m)$ space and processes events in $O(\log m)$ time. We then show that the movement of the Voronoi center c_{pqs} —the point equidistant to three sites $p, q, s \in S$ — can also change $O(m^3)$ times (Section 4). We again show that this bound is tight, and develop a compact, efficient, and responsive KDS to maintain c_{pqs} . The space usage is linear, and handling an event takes $O(\log^2 m)$ time. Both our KDSs can be made local as well, and therefore efficiently support updates to the movement of the sites. Building on these results we then analyze the full Voronoi diagram $\text{VD}_P(S)$ of n moving sites (Section 5). We identify the different types of events at which $\text{VD}_P(S)$ changes, and bound their number. Table 1 gives an overview of our bounds. We then develop a compact KDS to maintain $\text{VD}_P(S)$.

2 Preliminaries

We first review some properties of geodesic Voronoi diagrams and shortest path maps that we will use. Let SPM_s be the shortest path map of s , hence for all points in a region of SPM_s the shortest path from s has the same internal vertices. Each such region R is star-shaped with respect to the last internal vertex v on the shortest path. Often it will be useful to refine R into triangles incident to v . We refer to the resulting subdivision of P as the *extended* shortest path map. With some abuse of notation we will use SPM_s to denote this subdivision as well. An edge in SPM_s that starts in a vertex v that is colinear with the last edge in $\pi(s, v)$ is called an *extension segment* $E_{vs} = E_v$.

Let $\mathbb{T} = \mathbb{R}$ denote the time domain. We consider each site $s \in S$ as a function from \mathbb{T} to P . For functions we will not distinguish between the function itself and its graph. We say that a function is *simple* if it is continuous, i.e. if it has no break points.

Given two sites p and q , the bisector B_{pq} is the set of all points that are equidistant to p and q . If no vertex of P lies on the bisector, then B_{pq} is a piecewise curve connecting two points on ∂P . Each curve on the bisector is a subarc of a hyperbola that could degenerate to a segment [4, 18].

Lemma 1 (Aronov [4]). *$\text{VD}_P(S)$ consists of $O(n)$ vertices with degree 1 or 3, and $O(m)$ vertices of degree 2. For each degree 2 vertex v there is $p, q \in S$ so that v lies on the bisector B_{pq} and v lies on extension segment of SPM_p or SPM_q . All edges of $\text{VD}_P(S)$ are hyperbolic arc segments. Every vertex v of P contributes at most one extension segment E_v .*

Lemma 2 (Aronov et al. [3]). *Let s be a point moving linearly inside a simple polygon P with m vertices. The extended shortest path map SPM_s changes at most $O(m)$ times.*

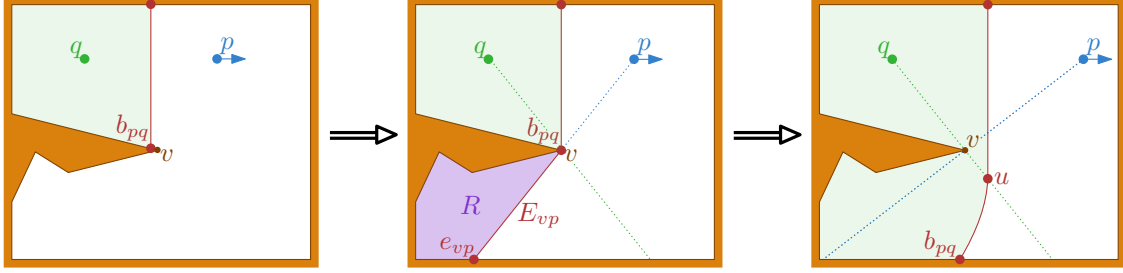


Fig. 3: A vertex event at v may coincide with a 1,2-expand event. At the time of the event all points in R are equidistant to p and q , and b_{pq} jumps from v to e_{vp} .

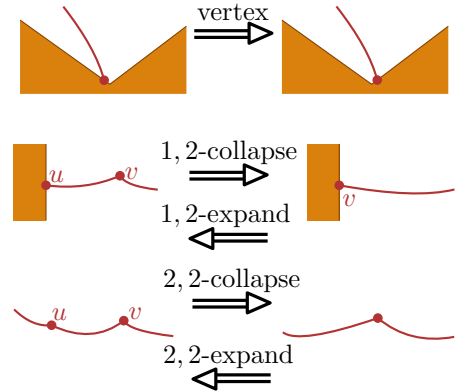
Lemma 3. *Let v be a vertex of P , there are $O(mn\beta_4(n))$ time intervals in which v has a unique closest site $s \in S$, and the distance from v to s over time is a hyperbolic function.*

Proof. For every site $s \in S$, consider the distance function $f_s(t) = \pi(s(t), v)$ from s to v . The site closest to v corresponds to the lower envelope of these n functions. Each function consists of $O(m)$ pieces in which the distance is a simple hyperbolic function. Since two such pieces can intersect at most twice this lower envelope has complexity $O(mn\beta_4(n))$ [25]. \square

3 A Single Bisector

Fix a pair of sites p and q , and let $b_{pq}(t)$ and $b_{qp}(t)$ be the endpoints of the bisector B_{pq} defined so that p lies to the right of $B_{pq}(t)$ when following the bisector from $b_{pq}(t)$ to $b_{qp}(t)$. As p and q move, the structure of B_{pq} changes at discrete times, or events. We distinguish between the following types of events (see Fig. 2):

- *vertex* events, at which an endpoint of B_{pq} coincides with a vertex of P ,
- *1,2-collapse* events, at which a degree 2 vertex (an interior vertex) of B_{pq} disappears as it collides with a degree 1 vertex (an endpoint),
- *1,2-expand* events, at which a new degree 2 vertex appears from a degree 1 vertex,
- *2,2-collapse* events at which a degree 2 vertex disappears by colliding with another degree 2 vertex,
- *2,2-expand* events, at which a new degree 2 vertex appears from a degree 2 vertex.



In Section 3.1 we prove that there are at most $O(m^2)$ vertex and 1,2-collapse events, and at most $O(m^3)$ 2,2-collapse events. The number of expand events can be similarly bounded. Some of these events may actually happen simultaneously. See for example Fig. 3, where B_{pq} changes when a vertex event and a 1,2-expand event coincide. Note that as a result, we are double-counting these simultaneous events. Despite this, we can show that our resulting $O(m^3)$ bound on the number of changes of B_{pq} is tight in the worst case. In Section 3.2 we then argue that there is a KDS that can maintain B_{pq} efficiently.

Fig. 2: The types of events at which the structure of B_{pq} changes.

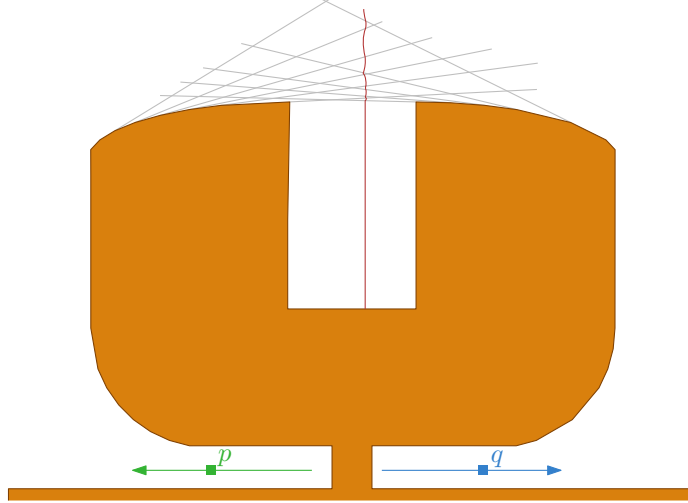


Fig. 4: The bisector B_{pq} may be involved in $\Omega(m^3)$ 2, 2-collapse events.

3.1 Bounding the Number of Events

We start by showing that a bisector may change $\Omega(m^3)$ times. We then argue that there is also an $O(m^3)$ upper bound on the number of such changes.

Lemma 4. *The bisector $B_{pq}(t)$ can change $\Omega(m^3)$ times.*

Proof. The main idea is to construct a bisector B_{pq} , a piecewise hyperbolic curve, of complexity $\Omega(m)$ in the middle of a region that consists of $\Omega(m^2)$ cells. These cells are defined by the extension segments in SPM_p and SPM_q that extend from the vertices on two convex chains of the polygon, one on either side of B_{pq} . See Fig. 4 for an illustration. Each cell defines a slightly different hyperbolic curve of the bisector, thus passing from one cell to another causes a change to the bisector. When one of the sites moves, the bisector sweeps over $\Omega(m^2)$ of these cells, causing $\Omega(m^2)$ changes to the bisector. The upper two convex chains of the polygon have complexity $\Omega(m)$ each and are placed in such a way that as p moves, B_{pq} moves to the right, sweeping the $\Omega(m^2)$ middle cells.

Next, we argue that B_{pq} can be moved back and forth across these cells $\Omega(m)$ times. By adding two convex chains to the bottom of the polygon, just above p and q , we can ensure that p and q alternate being the closest to the top of the polygon. Thus, when p is closest the bisector will move to the right and when q is the closest the bisector will move to the left. By making p and q move at the same speed and having the segments defining the convex chain on q 's side start and end in the middle of where the segments of the convex chain on p 's side, we can cause this alternation. When both of these lower convex chains have complexity $\Omega(m)$, the bisector sweeps over the $\Omega(m^2)$ middle cells $\Omega(m)$ times and thus the bisector changes $\Omega(m^3)$ times. \square

Lemma 5. *The bisector $B_{pq}(t)$ is involved in at most $O(m^2)$ vertex events.*

Proof. At a vertex event one of the endpoints of $B_{pq}(t)$, say $b_{pq}(t)$ coincides with a polygon vertex v . Hence, at such a time $\pi(p(t), b_{pq}(t)) = \pi(q(t), b_{pq}(t))$. The distance functions from p and q to v are piecewise hyperbolic functions with $O(m)$ pieces. So there are $O(m)$ time intervals during which both these distance functions are simple hyperbolic functions. A pair of such functions intersects at most a constant number of times. Hence, in each such interval there are at most $O(1)$ vertex events involving vertex v . The bound follows by summing over all time intervals and all vertices. \square

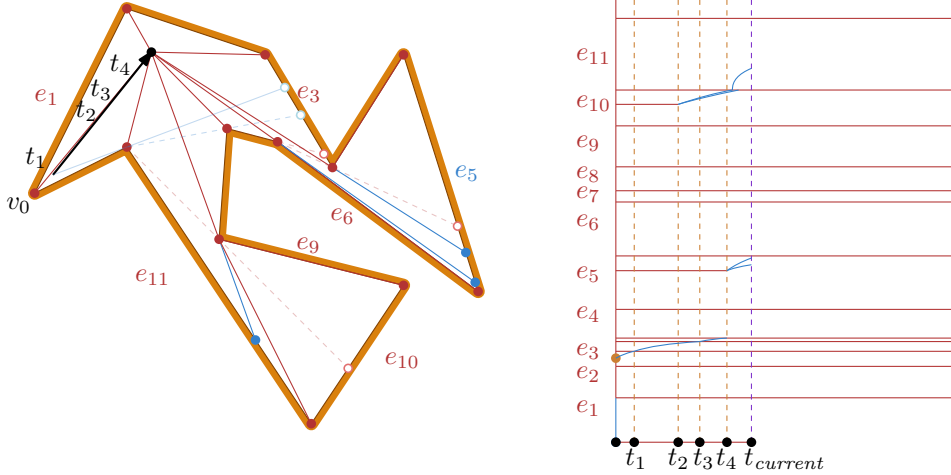


Fig. 5: Tracing $\text{SPM}_q(t) \cap \partial P$ as a function of t yields a subdivision \mathcal{S} .

Fix a polygon vertex v , and consider the extension segment $E_{vp}(t)$ in $\text{SPM}_p(t)$ incident to v . Let $e_{vp}(t)$ be the other endpoint of $E_{vp}(t)$, and observe that $e_{vp}(t)$ moves monotonically along the boundary of P . That is, as p moves, e_{vp} moves only clockwise along ∂P or only counter-clockwise. Hence, the trajectory of e_{vp} consists of $O(m)$ edges, on each of which e_{vp} moves along an edge of P .

Lemma 6. *Let v be a vertex of P . As p and q move, e_{vp} crosses $O(m)$ cells of SPM_q .*

Proof. Consider the intersection between $\text{SPM}_q(t)$ and ∂P as a function of t . This yields a planar subdivision \mathcal{S} of $\mathbb{T} \times \partial P$ of complexity $O(m)$ (Lemma 2). Observe that the edges of \mathcal{S} trace the trajectories of vertices of $\text{SPM}_q(t)$. We distinguish two types of vertices in $\text{SPM}_q(t)$, red vertices and blue vertices. The red vertices are either polygon vertices, or endpoints $e_{uq}(t)$ of extension segments for which $\pi(q(t), e_{uq}(t))$ contains at least one other polygon vertex. All other vertices—these correspond to endpoints $e_{wq}(t)$ of extension segments such that $\pi(q(t), e_{wq}(t)) = \|q(t)e_{wq}(t)\|$ —are blue. This coloring of the vertices of SPM_q also induces a coloring of the edges of \mathcal{S} . See Fig. 5. Since all red vertices have fixed locations, the corresponding red edges in \mathcal{S} are horizontal line segments. Furthermore, observe that every polygon edge is visible from $q(t)$ in a single time interval. Hence, there are at most two moving endpoints e_{wq} per polygon edge. This implies that every horizontal strip defined by two consecutive red edges contains at most two blue edges.

Finally, observe that the number of cells of SPM_q visited by e_{pv} corresponds to the number of faces of \mathcal{S} intersected by the curve representing the trajectory of e_{pv} . Since e_{pv} moves monotonically, this curve is t, λ -monotone. It follows that the total number of intersections with the red edges is $O(m)$. The edges in the trajectory of e_{pv} as well as the blue edges are curves of low algebraic degree, hence a pair of such curves intersect only $O(1)$ times. Moreover, using that every strip between two consecutive red edges contains at most two blue edges, that we have at most $O(m)$ such strips, and that e_{pv} has complexity $O(m)$ it follows that the total number of intersections between the trajectory of e_{pv} and the blue edges is only $O(m)$ in total. The lemma follows. \square

Lemma 7. *The bisector $B_{pq}(t)$ is involved in at most $O(m^2)$ 1, 2-collapse events.*

Proof. Fix a vertex v , and consider the endpoint $e_{vp}(t)$ of $E_{vp}(t)$. By Lemma 6 this point intersects at most $O(m)$ regions of SPM_p and SPM_q throughout the motion of p and q . It then follows that there are $O(m)$ time intervals during which the distances $f(t) = \pi(p(t), e_{vp}(t))$ and $g(t) = \pi(q(t), e_{vp}(t))$

are both simple and low algebraic degree. We restrict the domains of f and g to the time intervals during which p is closer to v than q . It follows that f and g still consist of $O(m)$ pieces.

Now observe that any 1, 2-collapse event of $B_{pq}(t)$ on $E_{vp}(t)$ corresponds to a time where: v is closer to p than q , and the endpoint $e_{vp}(t)$ of $E_{vp}(t)$ is equidistant to p and q , that is, $f(t) = g(t)$. Hence, the number of such events equals the number of intersections between (the graphs of) f and g . Since f and g both consist of $O(m)$ pieces, each of low algebraic degree, the number of intersections, and thus the number of 1, 2-collapse events on $E_{vp}(t)$ is $O(m)$. Similarly, the number of events on $E_{vq}(t)$ is $O(m)$. The lemma follows by summing these events over all vertices v . \square

Lemma 8. *The bisector $B_{pq}(t)$ is involved in at most $O(m^3)$ 2, 2-collapse events.*

Proof. We observe that in a 2, 2-collapse of edge (a, b) of $B_{pq}(t)$ both a and b must be on extension segments E_u and E_v in the shortest path map of p or q at time t . Hence a 2, 2-collapse occurs at the intersection point of E_u and E_v . In particular, at such an event, the distances from p to a and from q to a are equal.

If E_u and E_v both occur in a single shortest path map, say $\text{SPM}_p(t)$, this 2, 2-collapse event corresponds to an event at which the combinatorial structure of SPM_p changes. Thus, the total number of such changes is at most $O(m)$ (Lemma 2). We thus focus on the case that E_u is an extension segment in SPM_p and E_v is an extension segment in SPM_q .

Since the combinatorial structure of SPM_p and SPM_q changes at most $O(m)$ times, the total number of pairs of extension segments that we have to consider is $O(m^2)$. We now argue that for each such pair there are at most $O(m)$ times t where $\pi(p(t), a(t)) = \pi(q(t), a(t))$, and thus there are at most $O(m)$ 2, 2-collapse events involving the pair (E_u, E_v) . The total number of 2, 2-collapse events is then $O(m^3)$ as claimed.

The distance function from p to u is a piecewise hyperbolic function with $O(m)$ pieces. The same is true for the distance function from q to v . We then consider maximal time intervals during which both these distance functions are simple, and during which E_u and E_v are part of their respective shortest path maps. There are at most $O(m)$ such intervals. Since E_u and E_v move along a trajectory of constant complexity (i.e. they either rotate continuously around u and v , respectively, or remain static), the distance function $f(t, \mu) = \pi(p(t), u) + \|uE_v(\mu)\|$ from p via u to a point $E_v(\mu)$ on E_v also consists of $O(m)$ pieces, each of low algebraic degree. The same applies for the distance function $g(t, \lambda) = \pi(q(t), v) + \|vE_u(\lambda)\|$, for $E_u(\lambda)$ on E_u . Therefore, during each time interval, the distance functions from p to a and from q to a are also simple low-degree algebraic functions. Such functions intersect at most $O(1)$ times, and thus the number of 2, 2-collapse events in every interval is at most constant. Since we have $O(m)$ intervals, the number of 2, 2-collapses involving E_u and E_v is $O(m)$. \square

Theorem 9. *Let p and q be two points moving linearly inside P . The bisector B_{pq} of p and q can change $O(m^3)$ times. This bound is tight in the worst case.*

Proof. The bisector B_{pq} changes either at a vertex event, a 1, 2-collapse, or a 2, 2-collapse. By Lemmas 5, 7, and 8 there are at most $O(m^2)$, $O(m^2)$, and $O(m^3)$, such events respectively. We can use symmetric arguments to bound the expand events. Thus B_{pq} changes at most $O(m^3)$ times. By Lemma 4 this bound is tight in the worst case. \square

Even though the entire bisector B_{pq} may change $O(m^3)$ times in total, the trajectories of its intersection points with the boundary of P have complexity at most $O(m^2)$:

Lemma 10. *The trajectory of b_{pq} has $O(m^2)$ edges, each of which is a low-degree algebraic curve.*

Proof. The trajectory of b_{pq} changes only at vertex events or at 1,2-collapse events. By Lemmas 5 and 7 the number of such events is at most $O(m^2)$. Fix a time interval in between two consecutive events, and assume without loss of generality that $b_{pq}(t)$ moves on an edge of P that coincides with the x -axis. We thus have $b_{pq}(t) = (x(t), 0)$, for some function x . Since $\pi(p(t), b_{pq}(t)) = \pi(q(t), b_{pq}(t))$ we have that $\sqrt{Q_p(t)} + C_p + \sqrt{(x(t) - D_p)^2 + E_p} = \sqrt{Q_q(t)} + C_q + \sqrt{(x(t) - D_q)^2 + E_q}$, for some quadratic functions $Q_p(t)$ and $Q_q(t)$ and constants C_p, C_q, D_p, D_q, E_p , and E_q . By repeated squaring and basic algebraic manipulations it follows that $x(t)$ is some low degree algebraic function in t . Hence, every edge in the trajectory of b_{pq} corresponds to a low-degree algebraic curve. \square

3.2 A Kinetic Data Structure to Maintain a Bisector

We first describe a simple, yet naive, KDS to maintain B_{pq} that is not responsive and then show how to improve it to obtain a responsive KDS.

3.2.1 A Non-Responsive KDS to Maintain a Bisector

Our naive KDS for maintaining B_{pq} stores: (i) the extended shortest path maps of p and q using the data structure of Aronov et al. [3], (ii) the vertices of B_{pq} , ordered along B_{pq} from b_{pq} to b_{qp} in a balanced binary search tree, and (iii) for every vertex u of B_{pq} , the cell of SPM_p and of SPM_q that contains u . Since all cells in SPM_p and SPM_q are triangles, this requires only $O(1)$ certificates per vertex. We store these certificates in a priority queue \mathcal{Q} .

At any time where B_{pq} changes combinatorially (i.e. at an event) the shortest path to a vertex v of B_{pq} changes combinatorially, which indicates a change in the SPM cells that contain v . Hence, we detect all events. Conversely, when any vertex v of B_{pq} moves to a different SPM cell there is a combinatorial change in the bisector, so each event triggered by parts (ii) and (iii) of the KDS is an external event. The events at which SPM_p or SPM_q changes are internal (unless they also cause a combinatorial change in a shortest path to a vertex of B_{pq}).

The events at which SPM_p or SPM_q changes are handled as in Aronov et al. [3]. However, such an event may cause the shortest path to several bisector vertices to change and we would need to recompute the certificates for maintaining which cell of the SPM each bisector vertex lies in. The internal update for the SPM takes $O(\log m)$ time [3] and each certificate can be recomputed in $O(\log m)$ time by computing the appropriate distance functions. Unfortunately, there may be $\Theta(m)$ certificates to update, which means such an event may take $\Theta(m \log m)$ time. We will describe how to avoid this problem later, but we first describe how the rest of the events of the KDS are handled.

At any external event, a vertex u of B_{pq} leaves its cell in SPM_p or SPM_q , and enters a new one. In all cases we delete the $O(1)$ certificates corresponding to u , and replace them by $O(1)$ new ones. Depending on the type of event, we also update B_{pq} appropriately, i.e. in case of a 1,2- or 2,2-collapse event we remove a vertex from B_{pq} and in case of 1,2-expand events we insert a new vertex in B_{pq} . We describe how to handle a vertex event in more detail, as they may happen simultaneously with 1,2-collapse or expand events.

Consider a vertex event at vertex v at time t , at which a bisector endpoint, say b_{pq} , stops to intersect an edge \overline{wv} of ∂P .

If there are no points in P other than v for which the shortest path to p or q passes through v then the vertex event is easy to handle; at such an event b_{pq} simply moves onto the other edge incident to v . In doing so, it crosses into a different cell of SPM_p or SPM_q . So, we update the certificates associated with b_{pq} and continue to the next event.

If there are points r in some region $R \subset P$ for which $\pi(r, p)$ and $\pi(r, q)$ both pass through v , then these points are now all equidistant to p and q , and hence at time t the entire region R is actually a

subset of the bisector B_{pq} . See Fig. 3. This region R is bounded by the extension segment incident to v in SPM_p , or the extension segment incident to v in SPM_q , that is, E_{vp} or E_{vq} . As a result, the endpoint b_{pq} will jump to either e_{vp} or e_{vq} (the other endpoint of E_{vp} or E_{vq} , respectively). Moreover, this extension segment becomes part of the bisector B_{pq} in the simultaneously occurring 1, 2-expand event. This new vertex u of B_{pq} moves on the other extension segment incident to v . Hence, to update our KDS we insert a new vertex u in the balanced binary search tree representing B_{pq} , create the corresponding certificates tracking u in SPM_p and SPM_q , and we update the certificates tracking b_{pq} in SPM_p and SPM_q .

If there are points for which only one of the shortest paths to p or q , say p , passes through v , the bisector endpoint b_{pq} continues on the other edge incident to v , while a new vertex u is created on B_{pq} moving along E_{vp} . We insert u in B_{pq} and create appropriate certificates tracking u and b_{pq} in SPM_p and SPM_q like in the previous case.

Observe that we may also have vertex events at which a bisector endpoint b_{pq} jumps onto v while it was moving on an edge not incident to v before in a situation symmetric to in the second case described above. In such a case the vertex event coincides with a 1, 2-collapse event in which a bisector vertex u hits ∂P (and thus the boundary of its cell in SPM_p and SPM_q) at v . This is the reverse situation of the one depicted in Fig. 3. In this case we delete u and its certificates, and update the certificates tracking b_{pq} .

Each external event involves only a constant number of vertices of B_{pq} . Furthermore, as each such vertex is involved in only a constant number of certificates, each of which can easily be updated in $O(\log m)$ time, handling an external event can be done in $O(\log m)$ time.

Observe that at any moment we maintain only $O(m)$ certificates, stored in a priority queue. We thus use $O(m)$ space, and the updates to the priority queue require $O(\log m)$ time. The total number of events for maintaining SPM_p and SPM_q is only $O(m)$, which is dominated by the $O(m^3)$ events at which B_{pq} itself changes (Theorem 9). So our KDS is compact, and efficient, but not responsive as updates to the SPM may require $O(m \log m)$ time. In the next section we show that we do not actually need to maintain these certificates explicitly.

3.2.2 A Responsive KDS to Maintain a Bisector

First we dissect in some more detail the anatomy of a bisector. Each bisector consists of two endpoints which are degree 1 vertices and a chain of degree 2 vertices connecting them. We can further divide this chain based on which parts are directly visible from the sites defining the bisector. This division results in at most 5 pieces, as illustrated in Fig. 6; some pieces may not be present in every bisector. First there is a *double-visible* piece that is visible from both sites p and q . Since P is a simple polygon, this piece consists of a single line segment. Adjacent to the double-visible piece on either side there may be a *single-visible* piece that is only visible to p or to q , but not both. Lastly, there are up to two *non-visible* pieces that are not directly visible from either p or q .

We will still store the bisector vertices in a balanced binary tree ordered along the bisector, but we will store the certificates for the degree 2 vertices a little differently. For each of the at most four degree 2 vertices that separate

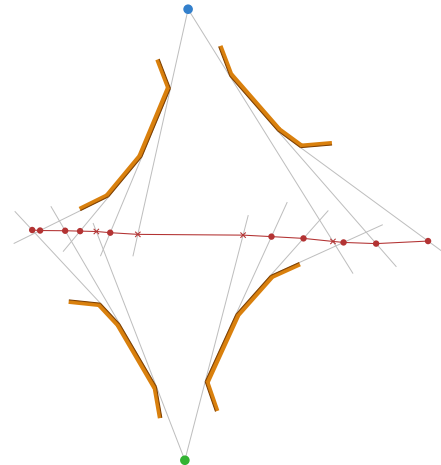


Fig. 6: A bisector can be split into at most five pieces, here separated by degree 2 vertices marked as crosses.

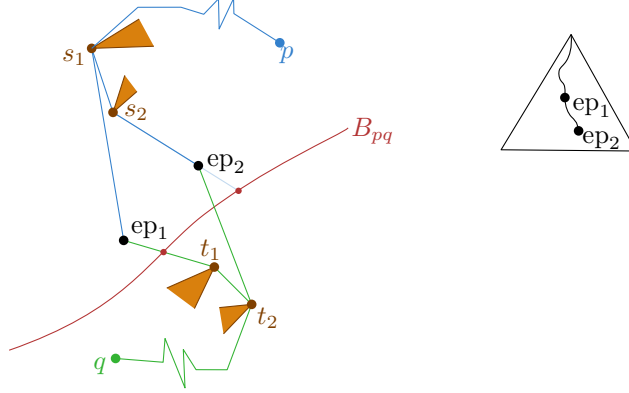


Fig. 7: On the left is a schematic drawing of the event points ep_1 and ep_2 with their shortest paths towards p and q . On the right how (the certificates of) ep_1 and ep_2 are stored in the BST.

the pieces as well as the degree 1 endpoints, we store the cells of SPM_p and SPM_q contain it. Then we observe that for internal vertices of the single-visible piece there can be no events. Each of these internal vertices lies on an extension segment of a single convex chain of vertices in the simple polygon and these extension segments do not intersect. Therefore no 2,2-collapses can occur.

The non-visible pieces are trickier, since 2,2-collapses may occur when a vertex moving on an extension segment of SPM_q moves to a different cell of SPM_p . Fortunately such potential events on a single non-visible bisector piece are related and form a strict ordering, regardless of the exact distance functions of the various vertices to p and q .

We define event points to be the locations at which 2,2-collapses that may occur. Consider two degree 2 vertices v and w that are internal to a non-visible piece of bisector between sites p and q , such that v and w are adjacent on the bisector and we have that v is on an extension segment of SPM_p and w is on an extension segment of SPM_q . Let the *event point* $ep_{v,w}$ denote the intersection between these two extension segments. A 2,2-event between v and w corresponds to the event point being on the bisector between p and q . Without loss of generality assume that the event point currently lies in the Voronoi cell of p . We can then use the certificate $\pi(ep_{v,w}, p) < \pi(ep_{v,w}, q)$ to detect the 2,2-event between v and w . As we saw above maintaining these certificates explicitly is not efficient as any change in the shortest path towards p or q requires us to recompute the failure time. Instead we will store all event points in the Voronoi cell of p in one balanced binary tree ordered along the bisector and those in q in another. For each node in such a tree, we maintain the event point in its subtree that will be the first to be on the bisector, similar to a kinetic tournament where internal nodes store additional values. We then compute an explicit failure time only for the two event points stored in the roots of the trees.

For a single non-visible bisector piece between sites p and q , Consider event points ep_1 and ep_2 where ep_2 is a child of ep_1 in the tree. Let s_1 and t_1 denote the first polygon vertex on the shortest path from ep_1 towards p and q respectively and let s_2 and t_2 be defined symmetrically. See Fig. 7. Then we can rewrite the certificate for ep_1 as

$$\pi(ep_1, s_1) + \pi(s_1, p) < \pi(ep_1, t_1) + \pi(t_1, q) \quad \equiv \quad \pi(ep_1, s_1) - \pi(ep_1, t_1) < \pi(t_1, q) - \pi(s_1, p),$$

and the certificate for ep_2 similarly. Then observe that if $s_1 = s_2$ and $t_1 = t_2$, then ep_1 will be on the bisector before ep_2 if and only if $\pi(ep_1, s_1) - \pi(ep_1, t_1) > \pi(ep_2, s_2) - \pi(ep_2, t_2)$. This creates a strict ordering of the event points in the Voronoi cell of p . Unfortunately in many cases the first vertex on the path towards p or q will not be the same for every vertex on the bisector. Therefore

we introduce an offset value to allow comparing event points that have different first vertices on their paths towards p and q .

If $s_1 \neq s_2$ and $t_1 \neq t_2$, we should compare based on a common node on the paths towards p and q , which may be any combination of s_1 or s_2 and t_1 or t_2 . As these cases are analogous, we consider the case where s_1 and t_2 are on the shortest paths towards p and q respectively for both event points. (Intuitively s_1 and t_2 are further towards p and q .)

Now the values we would like to compare are

$$\pi(\text{ep}_1, s_1) - \pi(\text{ep}_1, t_2) > \pi(\text{ep}_2, s_1) - \pi(\text{ep}_2, t_2).$$

However these are not what we stored. With some rewriting, we find that the above inequality holds if and only if

$$\pi(\text{ep}_1, s_1) - \pi(\text{ep}_1, t_1) > \pi(\text{ep}_2, s_2) - \pi(\text{ep}_2, t_2) - \pi(s_1, s_2) - \pi(t_1, t_2).$$

We call $-\pi(s_1, s_2) - \pi(t_1, t_2)$ the offset of ep_2 with respect to ep_1 . Now each node will store the maximum event value in its subtree as follows. For a leaf the maximum is its own event value. For an internal node, it is the maximum over its own event value and the maximum values of its children with the offset added. The maximum value stored at the root can then be used to determine the first time an $2, 2$ -event happens among the bisector vertices stored in the tree.

Note that the above data structure stores only a constant number of certificates directly involving p or q , all of which are stored at the root of the tree. Therefore, it can be made to support changes in the movement of p and q in $O(\log m)$ time. Furthermore, we can support splitting the bisector at a vertex in $O(\log^2 m)$ time, since a split affects $O(\log m)$ nodes in the balanced binary search tree, and recomputing the offsets (and thus updating the certificates) takes $O(\log m)$ time per node.

By replacing part (iii) of the naive structure with this data-structure we are still guaranteed to detect all events, but now when SPM_p changes, we have to update only a constant number of certificates (rather than $\Theta(m)$). As the certificates are stored in a binary tree it is easy to add or remove vertices when the bisector is expanded or shrinks. This provides us with the following Theorem:

Theorem 11. *Let p and q be two sites moving linearly inside a simple polygon P with m vertices. There is a KDS that maintains the bisector B_{pq} that uses $O(m)$ space and processes at most $O(m^3)$ events, each of which can be handled in $O(\log m)$ time. Additionally it can support movement changes of p and q in $O(\log m)$ time and splitting the bisector at any given vertex in $O(\log^2 m)$ time.*

4 A Voronoi Center

Let $c_{pqs}(t)$ be the point equidistant to $p(t)$, $q(t)$, and $s(t)$ if it exists. By Aronov et al. [5] (Lemma 2.3.5) there is indeed at most one such a point. We refer to c_{pqs} as the *Voronoi center* of p , q , and s . Note that there may be times at which c_{pqs} does not exist. We identify five types of events at which c_{pqs} may appear or disappear, or at which the movement of c_{pqs} can change (see Fig. 8). They are:

- *1, 3-collapse* events in which c_{pqs} collides with the boundary of the polygon (in a bisector endpoint) and disappears from P ,
- *1, 3-expand* events in which c_{pqs} appears on the boundary of P as two bisector endpoints intersect, creating a point equidistant to all three sites,
- *vertex-events* where c_{pqs} appears or disappears strictly inside P , as two sites, say p and q , are equidistant to a vertex v that appears on the shortest paths to c_{pqs} ,

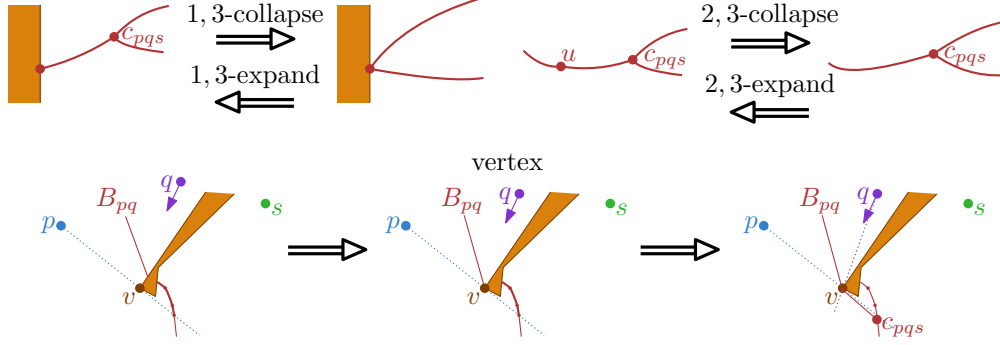


Fig. 8: The events that can happen during the movement of a Voronoi center.

- 2,3-collapse events where one of the geodesics from either p , q , or s to c_{pqs} loses a vertex,
- 2,3-expand events where one of the shortest paths gains a new vertex.

Observe that, as the name suggests, at a 1,3-collapse event the Voronoi center (a degree 3 vertex in $\text{VD}_P(\{p, q, s\})$) disappears as it collides with the endpoint of a bisector (a degree 1 vertex). Similarly, at a 2,3-collapse event a degree 2 vertex on one of the bisectors disappears as it collides with a degree 3 vertex (the Voronoi center c_{pqs}). As in case of the bisector, some of these events may coincide. In the next section, we bound the number of events, and thus the complexity of the trajectory of c_{pqs} . We then present a kinetic data structure to maintain c_{pqs} in Section 4.2.

4.1 Bounding the Number of Events

We give a construction in which the trajectory of c_{pqs} has complexity $\Omega(m^3)$, and then prove a matching upper bound.

Lemma 12. *The trajectory of the Voronoi center c_{pqs} of three points p , q , and s , each moving linearly, may have complexity $\Omega(m^3)$.*

Proof. The main idea is that we can construct a trajectory for c_{pqs} of complexity $\Omega(m^2)$, even when two of the three sites, say p and q , are static. We place p and q so that their bisector B_{pq} , a piecewise hyperbolic curve of complexity $\Omega(m)$, intersects an (almost) horizontal line E $\Omega(m)$ times. We can realize this using two convex chains F_p and F_q in ∂P . See Fig. 9 for an illustration. We now construct a third convex chain D_s in ∂P and place the third site s so that the extension segments in SPM_s incident to the vertices of D_s all lie very close to E . Thus, each such segment intersects B_{pq} $\Omega(m)$ times. We choose the initial distances so that the voronoi center c_{pqs} lies on the rightmost segment of B_{pq} . Now observe that as s moves away from D_s , the center $c_{pqs}(t)$ will move to the left on B_{pq} , and thus it will pass over all $\Omega(m^2)$ intersection points of B_{pq} with the extension segments of the vertices in D_s . At each such time, the structure of one of the shortest paths $\pi(p(t), c_{pqs}(t))$, $\pi(q(t), c_{pqs}(t))$, or $\pi(s(t), c_{pqs}(t))$ changes (they gain or lose a vertex from F_p , F_q , or D_s , respectively). Hence, the trajectory of c_{pqs} changes $\Omega(m^2)$ times.

Next, we argue that we can make c_{pqs} “swing” back and forth $\Omega(m)$ times by having p and q move as well. The voronoi center c_{pqs} will then encounter every intersection point on B_{pq} $\Omega(m)$ times. It follows that the complexity of the trajectory of c_{pqs} is $\Omega(m^3)$ as claimed.

The idea is to add two additional convex chains, C_s and C_p , that make the bisector B_{ps} between p and s “zigzag” $\Omega(m)$ times throughout the movement of p and s . We can achieve this using a similar construction as in Lemma 4. To make sure that the bisector $B_{pq} = B_{pq}(t)$ between p and q

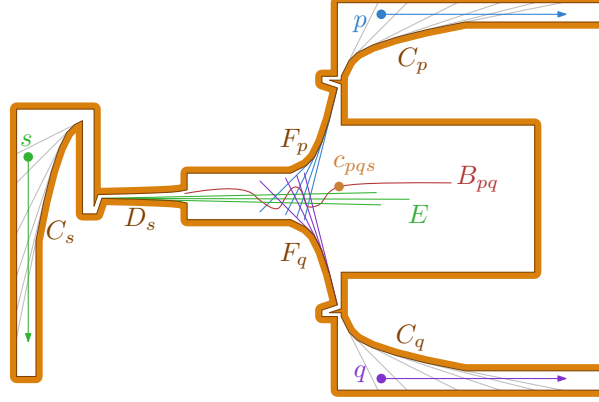


Fig. 9: A polygon in which the trajectory of a voronoi center c_{pqs} has complexity $\Omega(m^3)$.

remains static, we create a third chain C_q , which is a mirrored copy of C_p , and we make q move along a trajectory identical to that of p . See Fig. 9. Finally, observe that $c_{pqs}(t) = B_{pq} \cap B_{ps}(t)$, and thus $c_{pqs}(t)$ will indeed encounter all $\Omega(m^2)$ intersection points on B_{pq} $\Omega(m)$ times. The lemma follows. \square

Lemma 13. *The number of 1,3-collapse events is at most $O(m^2)$.*

Proof. At a 1,3-event c_{pqs} to exits the polygon. Observe that at such a time t a pair of bisector endpoints, say $b_{pq}(t)$ and $b_{ps}(t)$, intersect. By Lemma 10 the trajectories of b_{pq} and b_{ps} have $O(m^2)$ edges, each of which is a low-degree algebraic curve. Thus, there are $O(m^2)$ time intervals during which both b_{pq} and b_{ps} move along the boundary of P , and their movement is described by a low-degree algebraic function. So such a time interval, b_{pq} and b_{ps} coincide only $O(1)$ times. It follows that the total number of 1,3-collapse events involving p , q , and s is $O(m^2)$. \square

Lemma 14. *The number of vertex events is at most $O(m^2)$.*

Proof. Fix a vertex v and a pair of sites p, q . By Lemma 3 the site among p, q closest to v can change at most $O(m)$ times. Therefore, v can produce at most $O(m)$ vertex events due to the pair p, q . Summing over all m vertices and all $O(1)$ pairs gives us an $O(m^2)$ bound. \square

Theorem 15. *The trajectory of the voronoi center c_{pqs} has complexity $O(m^3)$. Each edge is a constant degree algebraic curve.*

Proof. A vertex in the trajectory of c_{pqs} corresponds to either a 1,3-collapse or expand, a vertex event, or a 2,3-collapse or expand. By Lemma 13 the number of 1,3-collapse events, and symmetrically, the number of 1,3-expand events, is $O(m^2)$. By Lemma 14 the number of vertex events is also $O(m^2)$. We now bound the number of 2,3-collapse (and symmetrically 2,3-expand) events by $O(m^3)$. Each such an event corresponds to a breakpoint in the distance function between c_{pqs} and one of the three sites. Hence, at such a time t , c_{pqs} leaves an (extended) shortest path map cell C_p in one of the three shortest path maps, say SPM_p , and enters a neighboring cell of SPM_p . Let C_q and C_s be the extended shortest path map cells in SPM_q and SPM_s , respectively, containing $c_{pqs}(t)$.

All cells in the (extended) shortest path map of p are triangles, and the map changes only $O(m)$ times throughout the movement of p (Lemma 2). Hence, C_p corresponds to a constant complexity region C'_p in $P \times \mathbb{T}$ whose boundaries are formed by constant degree algebraic surfaces, and there are $O(m)$ such regions in total. Similarly, we have $O(m)$ choices for the constant complexity regions

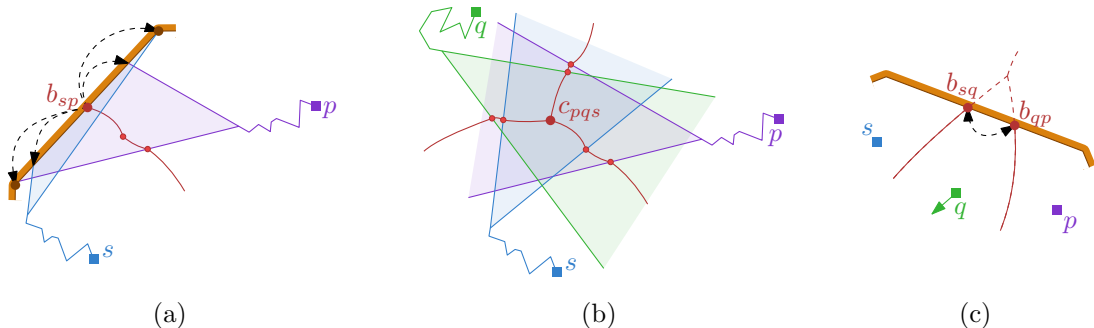


Fig. 10: In black the certificates that we maintain in order to detect: (a) events where b_{sp} changes movement, (b) 1,3-collapse, 2,3-collapse and 2,3-expand events, and (c) 1,3-expand events.

C'_q and C'_s corresponding to C_q and C_s . Observe that within $C'_p \cap C'_q \cap C'_s$, all points have the same combinatorial shortest paths to p , q , and s , and thus the distance functions are simple hyperbolic functions. Given these distance functions, the trajectory of c_{pqs} is a constant degree algebraic curve. Such a curve can intersect the boundary of $C'_p \cap C'_q \cap C'_s$ at most $O(1)$ times. It follows that the maximum complexity of c_{pqs} is thus $O(m^3)$. \square

4.2 A Kinetic Data Structure to Maintain a Voronoi Center

Our KDS for maintaining c_{pqs} stores: (i) the extended shortest path maps of p , q , and s , (ii) the cells of these shortest path maps containing c_{pqs} (when c_{pqs} lies inside P), and (iii) the endpoints of all bisectors (for all pairs), and their cyclic order on ∂P . In particular, for each such endpoint b_{sp} we keep track of the cells of SPM_p and SPM_s that contain it. See Fig. 10 for an illustration. At any time we maintain $O(m)$ certificates, which we store in a global priority queue.

Observe that at 1,3-collapse, 2,3-collapse, and 2,3-expand events the shortest path from c_{pqs} to one of the sites changes combinatorially. Hence, we can successfully detect all such events. At a vertex event a vertex is equidistant to two sites, say p and q . At such a time, one of the two endpoints of B_{pq} leaves an edge of P , and thus exits a shortest path map cell in SPM_p (and SPM_q). Since we explicitly track all bisector endpoints, we can thus detect this vertex event of c_{pqs} . Finally, at every 1,3-expand event two such bisector endpoints collide, and thus change their cyclic order along ∂P . We detect such events due to certificates of type (iii).

Any time at which c_{pqs} changes cells in a shortest path map results in a combinatorial change of its movement. Hence, any failure of a certificate of type (ii) is an external event (a 1,3-collapse, 2,3-collapse, or 2,3-expand). The certificates of types (i) and (iii) may be internal or external.

Theorem 16. *Let p, q and s be three sites moving linearly inside a simple polygon P with m vertices. There is a KDS that maintains the Voronoi center c_{pqs} that uses $O(m)$ space and processes at most $O(m^3)$ events, each of which can be handled in $O(\log^2 m)$ time. Updates to the movement of p, q , and s , can be handled in $O(\log^2 m)$ time.*

Proof. Certificate failures of type (i) are handled exactly as described by Aronov et al. [3]. This takes $O(\log^2 m)$ time. Note that changes to the shortest path maps may affect the certificates that guarantee that c_{pqs} or a bisector endpoint lies in a particular SPM cell. In these cases we trigger a type (ii) or type (iii) certificate failure. At a certificate failure of type (ii) at which c_{pqs} exits a shortest path map cell, we remove all certificates of type (ii) from the event queue. Next, for each site p, q , and s , we compute the new cell in the shortest path map containing c_{pqs} (if c_{pqs} still lies inside P). Finally, we create the appropriate new type (ii) certificates. Since all cells have constant

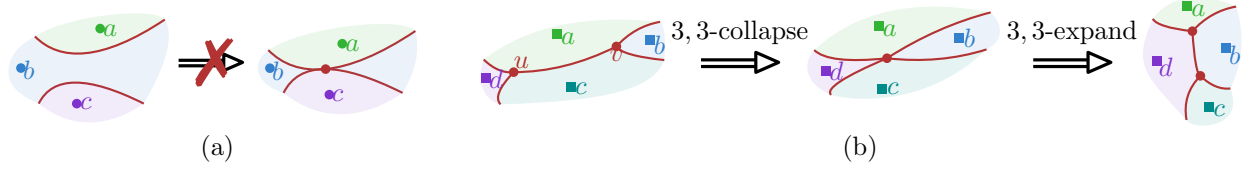


Fig. 11: (a) Voronoi edges cannot intersect in their interior. (b) The 3,3-collapse/expand events.

complexity, the total number of certificates affected is also $O(1)$. Computing them can easily be done in $O(\log^2 m)$ time.

Certificate failures of type (iii) where the movement of a bisector endpoint changes are handled using the same approach as in Section 3.2. Furthermore, at such an event we check if c_{pqs} appears or disappears, that is, if the event is actually a vertex event of c_{pqs} . This can be done in $O(\log^2 m)$ time [20]. If c_{pqs} disappears then we delete all type (ii) certificates. If c_{pqs} appears then we locate the cell of SPM_p , of SPM_q , and of SPM_s that contains c_{pqs} , and insert new type (ii) certificates that certify this. Finding the cells and updating the certificates can be done in $O(\log^2 m)$ time. At a certificate failure of type (iii) where two bisector endpoints collide, we check if the intersection point is equidistant to all three sites, and is thus a 1,3-expand event. Similarly to the approach described above, we add new type (ii) certificates in this case. Again this takes $O(\log^2 m)$ time.

Maintaining the extended shortest path maps requires handling $O(m)$ events [3]. Events where c_{pqs} crosses a boundary of an extended SPM correspond to changes in the trajectory of c_{pqs} . By Theorem 15 there are at most $O(m^3)$ such events. This dominates the $O(m^2)$ events that we have to handle to maintain the bisector endpoints in cyclic order around ∂P (Lemmas 10 and 13).

Since in addition to SPM_p , SPM_q , and SPM_s , we maintain only a constant amount of extra information. Since the KDS to maintain such a shortest path map SPM_s is local and can be updated to changes in the movement of s in $O(\log^2 m)$ time. The same applies for our data structure as well. We therefore obtain a compact, responsive, local, and efficient KDS. \square

5 The Geodesic Voronoi Diagram

In this section we consider maintaining the geodesic Voronoi diagram $\text{VD}_P(S)$ as the sites in S move. As a result of the sites in S moving, the Voronoi vertices and edges in $\text{VD}_P(S)$ will also move. However, we observe that all events involving Voronoi edges involve their endpoints; two edges cannot start to intersect in their interior as this would split a Voronoi region, see Fig. 11(a). Similarly, the interior of a Voronoi edge cannot start to intersect the polygon boundary. This means we can distinguish the following types of events that change the combinatorial structure of the Voronoi diagram.

- Edge collapses, at which an edge between vertices u and v shrinks to length zero. Let d_u, d_v , with $d_u \leq d_v$, be the degrees of u and v , respectively. We then have a d_u, d_v -collapse.
- Edge expands. These are symmetric to edge collapses.
- Vertex events, where a degree 1 vertex of $\text{VD}_P(S)$ crosses over a polygon vertex.

Indeed, we have seen most of these events when maintaining an individual bisector or Voronoi center (a degree 3 vertex in $\text{VD}_P(S)$). The only new types of events are the 3,3-collapse and 3,3-expand events which involve two degree 3 vertices. They are depicted in Fig. 11.(b). We again note that some of these events may happen simultaneously.

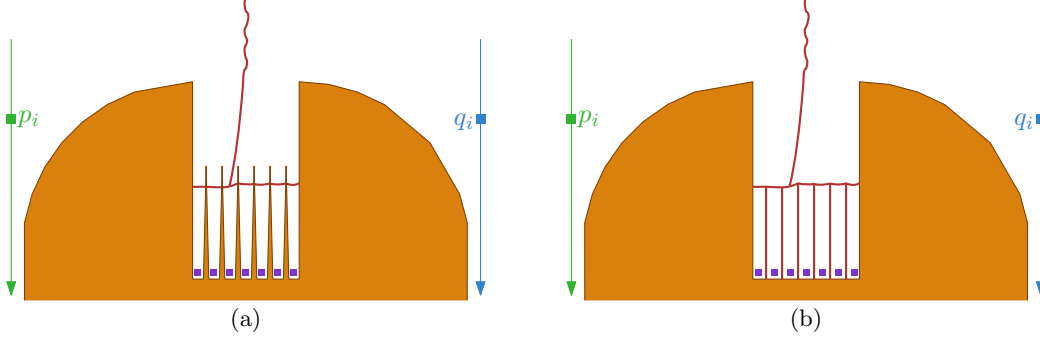


Fig. 12: The construction that yields $\Omega(nm \min\{n, m\})$ 1, 3-collapse events (a), and $\Omega(mn^2)$ 3, 3-collapse events (b).

Theorem 17. *Let S be a set of n sites moving linearly inside a simple polygon P with m vertices. During the movement of the sites in S , the combinatorial structure of the geodesic Voronoi diagram $\text{VD}_P(S)$ changes at most $O(m^3 n^3 \beta_z(n))$ times. In particular, the events at which $\text{VD}_P(S)$ changes, and the number of such events, are listed in Table 1.*

We prove these bounds in Section 5.1. For most of the lower bounds we generalize the constructions from Sections 3 and 4. For the upper bounds we typically fix a site or vertex (or both), and map the remaining sites to a set of functions in which we are interested in the lower envelope. In Section 5.8 we develop a kinetic data structure to maintain $\text{VD}_P(S)$.

5.1 Bounding the Number of Events

We analyze the number of collapse events and the number of vertex events. The expand events are symmetric to the collapse events.

5.2 1,2-collapse Events

Lemma 18. *There may be $\Omega(m^2 n)$ 1, 2-collapse events.*

Proof. See Fig. 18. Place $\Omega(m)$ “T-shaped” obstacles at the bottom of the pit. Now consider the ray from the left endpoint r of the top right chain through the top-left vertex v of a T-shaped obstacle. Let a be the point where this ray hits the floor of the pit. The site closest to a changes $\Omega(m)$ times from p_i to q_i (as the endpoint of the bisector sweeps from right to left). Every such a time corresponds to a 1, 2-collapse event. The lemma follows. \square

Lemma 19. *The number of 1, 2-collapse events is at most $O(m^2 n^2)$.*

Proof. Any 1, 2-collapse event in the Voronoi diagram uniquely corresponds to a 1, 2-collapse event of a bisector $B_{pq}(t)$ for some sites $p, q \in S$. By Lemma 7 the number of 1, 2-collapse events in $B_{pq}(t)$ is $O(m^2)$. The lemma follows by summing over all pairs $p, q \in S$. \square

5.3 1,3-collapse Events

Lemma 20. *There may be $\Omega(mn \min\{n, m\})$ 1, 3-collapse events.*

Proof. See Fig. 12(a). Place $\Omega(\min\{n, m\})$ spikes at the bottom of the pit and place a site between them. As two sites p_i and q_i move down, their bisector sweeps over all spikes causing the voronoi

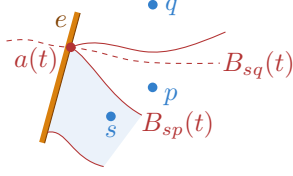


Fig. 13: At 1, 3-collapse event two bisector endpoints $b_{sp}(t)$ and $b_{sq}(t)$ meet.

center of p_i, q_i and the site between the spikes as the bisector to hit the side of each spike, causing a 1, 3-collapse event each time. Since the upper convex chains of the polygon consist of $\Omega(m)$ vertices, every pair of vertices causes $\Omega(m \min\{n, m\})$ such events. Note that while the horizontal part of the bisectors between the spikes moves up as a pair of vertices moves down, it “resets” when a new pair arrives, thus this process can be repeated $\Omega(n)$ times using new sites each time and the lemma follows. \square

By Lemma 13 any triple p, q, s generates at most $O(m^2)$ 1, 3-collapse events. So, summing over all triples this immediately gives us an $O(m^2 n^3)$ upper bound. Next, we argue that we can also bound the number of 1, 3-collapses by $O(m^3 n^2 \beta_z(n))$, for some $z \in \mathbb{N}$.

Lemma 21. *The number of 1, 3-collapse events is at most $O(m^3 n^2 \beta_z(n))$.*

Proof. Fix a site s and an edge e of the polygon. We now bound the number of 1, 3-collapse events on site e involving site s by $O(m^2 n \beta_z(n))$, for some constant z . Since we have n sites and m edges, the lemma then follows. At any time t , the Voronoi region of s intersects e in at most a single connected interval [1]. All 1, 3-events on e involving s occur on one of the two endpoints of this interval. Let $a(t)$ be the endpoint such that s lies right of the edge of $\text{VD}(t)$ that starts in $a(t)$. See Fig. 13. Next, we bound the number of events occurring at $u(t)$. Bounding the number of events occurring at the other endpoints is analogous. Observe that $a(t)$ is a bisector endpoint $b_{sp}(t)$ for some site p . More specifically, it is the “lowest” such endpoint along e . At an 1, 3-collapse event, the site that defines this “lowest” endpoint changes, that is, two bisector endpoints $b_{sp}(t)$ and $b_{sq}(t)$ meet. More formally, let $e = \overline{uv}$ and let $\lambda(w) \in [0, 1]$ be the value such that $w = (1 - \lambda(w))u + \lambda(w)v$ for all points $w \in e$. For a site r we then define the function

$$f_r(t) = \begin{cases} \lambda(b_{sr}(t)) & \text{if } b_{sr}(t) \text{ lies on } e \\ \perp & \text{otherwise.} \end{cases}$$

It now follows that a 1, 3-collapse event at $a(t)$ corresponds to a vertex in the lower envelope $\mathcal{L}(\{f_r \mid r \in (S \setminus \{s\})\})$. Since the trajectory of any b_{sr} has complexity $O(m^2)$ whose edges are low-degree algebraic curves (Lemma 10) that pairwise intersect $O(1)$ times, the same applies for function f_r . It follows that their lower envelope has complexity $O(m^2 n \beta_z(n))$, for some constant z , and thus the number of 1, 3-collapses at $u(t)$ is at most $O(m^2 n \beta_z(n))$ as well. \square

Corollary 22. *The number of 1, 3-collapse events is at most $O(m^2 n^2 \min\{m \beta_z(n), n\})$.*

5.4 2,2-collapse Events

Lemma 23. *There may be $\Omega(m^3 n)$ 2, 2-collapse events.*

Proof. We use the construction from Lemma 4 in which the bisector of a single pair of sites (p, q) changes $\Omega(m^3)$ times. We now simply create $\Omega(n)$ such pairs (p_i, q_i) that all move along the same

trajectories. We choose the starting positions such that the distance between two consecutive points p_i and p_{i+1} (q_i and q_{i+1}) is very large, so that for each pair (p_i, q_i) the bisector appears in the Voronoi diagram at the time when p_i and q_i pass by our construction. \square

Lemma 24. *The number of 2,2-collapse events is at most $O(m^3n\beta_4(n))$.*

Proof. Fix two vertices u and v . By Lemma 3 there are a total of $O(mn\beta_4(n))$ maximal time intervals during which both u and v have unique closest sites, and the distances from u and v to their respective closest sites, say r and s , is a simple hyperbolic function. Consider such an interval I , and observe that during I , there is only a single extension segment E_{ur} in the (non extended) SPM_r , and thus in VD, incident to u . Similarly, there is a single extension segment E_{vs} in VD incident to v . Like in Lemma 8, we now have that in I the distances from r and s to the intersection point of E_{ur} and E_{vs} are both simple algebraic functions of low degree. These functions intersect only a constant number of times, and thus there are at most $O(1)$ 2,2-collapse events per interval. In total we thus have $O(mn\beta_4(n))$ events per pair, and $O(m^3n\beta_4(n))$ events in total. \square

5.5 2,3-collapse Events

Lemma 25. *There may be $\Omega(mn^2 + m^3n)$ 2,3-collapse-events.*

Proof. We give two constructions. The first one gives $\Omega(m^3n)$ 2,3-collapse events and the second one $\Omega(mn^2)$. The lemma then follows.

For the first construction we modify the construction in Fig. 9 slightly. The main idea is that each time the Voronoi center moves into a new cell defined by F_p , F_q , and D_s a 2,3-collapse event occurs. Thus for three sites, we get $\Omega(m^3)$ such events. When we repeat this process by moving $\Omega(n)$ triples along the trajectories of p , q , and s , the first part of the lower bound follows. In order to do this, we modify the polygon by adding two horizontal rectangles, one to the left of p and one to the left of q , and a vertical rectangle, above s . These rectangles contain (the trajectories of) the future triples. By making the convex chains C_p , C_q , and C_s steep enough, we can ensure that all events occur close enough together, limiting how long the horizontal rectangles need to be, meaning that they do not overlap the vertical path of s , and thus maintaining a simple polygon.

The second construction is sketched in Fig. 14. We again have an obstacle with a convex chain of complexity $\Omega(m)$. On the left side of this obstacle, we have $\Omega(n)$ fixed sites. The bisectors of adjacent sites and the lines extending the edges of the convex chain form a grid of complexity $\Omega(mn)$. On the right side of the obstacle, we drop a site q_i such that the bisector of q_i and the fixed sites sweeps over the entire grid, causing $\Omega(nm)$ 2,3-collapse events. By dropping $\Omega(n)$ sites sufficiently far apart, we can repeat this process $\Omega(n)$ times, leading to the second part of the lower bound. \square

Consider an extension segment $E_{vp}(t)$ of $\text{SPM}_p(t)$ incident to v and let $\lambda \in [0, 1]$ be some linear parameter along $E_{vp}(t)$ such that $E_{vp}(t, \lambda) = (1 - \lambda)v + \lambda e_{vp}(t)$ is a point along $E_{vp}(t)$. Let $f_{vp,q}(t, \lambda) = \pi(q(t), E_{vp}(t, \lambda))$ denote the distance function from a site $q(t)$ to $E_{vp}(t, \lambda)$.

Lemma 26. *Consider a time interval in which SPM_q has fixed combinatorial structure. The function $f_{vp,q}$ restricted to this interval is a bivariate piecewise low-degree algebraic function of complexity $O(m)$.*

Proof. Every cell of SPM_q has constant complexity. Moreover, the function describing the movement of E has constant complexity as well. In particular, this function consists of at most three pieces, in at most one of which E lies on the (rotating) line through p and v , and in the other two E has a fixed location. It follows that each SPM_q cell contributes constant complexity to $f_{vp,q}$. Since there

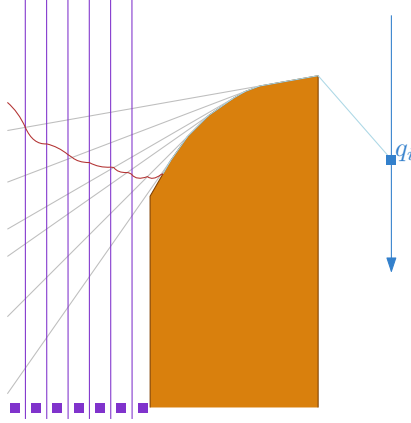


Fig. 14: An illustration of the construction that yields $\Omega(mn^2)$ 2,3-collapse events.

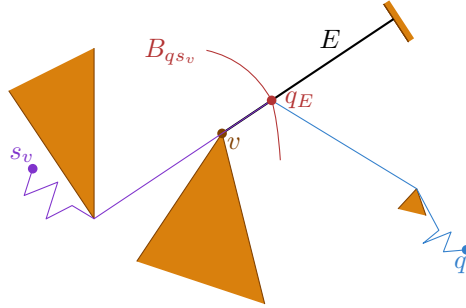


Fig. 15: The extension segment E incident to v defined by the site s_v closest to v , and the intersection point q_E between E and the bisector of q and s_v . The function g_q measures the distance from q_E to s_v , that is, the length of the red and blue paths.

are only $O(m)$ cells, the total complexity of $f_{vp,q}$ is at most $O(m)$. Every patch of $f_{vp,q}$ represents the Euclidean distance of a fixed point (a polygon vertex) to a points on a line rotating through v . This can be described by a low-degree algebraic function. \square

Lemma 27. *The number of 2,3-collapse events is at most $O(m^3n^2\beta_4(n)\beta_z(n))$.*

Proof. Any 2,3-collapse event at some time t occurs on an extension segment $E(t)$ incident to a polygon vertex v . In particular, $E(t)$ is an extension segment of the shortest path map of the site $s_v(t)$ which is closest to v at time t . Furthermore, by Lemma 1, v has only one such an extension segment at any time. We can thus charge the 2,3-event to v . We now bound the number of such charges to a vertex v by $O(m^2n^2\beta_4(n))$. The lemma then follows.

Split time into time intervals in which: (i) the site $s_v(t)$ closest to v is fixed, and the distance from $s_v(t)$ to v is a simple hyperbolic function, and (ii) the shortest path maps from all sites have a fixed combinatorial structure. It follows from Lemmas 2 and 3 that there are $O(mn\beta_4(n))$ intervals in total.

Fix such a time interval I . For any (other) site $q \neq s_v$, let $q_E(t)$ be the intersection point of $E(t)$ and the bisector of q and $s_v(t)$. See Fig. 15. The distance function $f_{E,q}$ restricted to I has complexity $O(m)$ (Lemma 26), and the distance from $s_v(t)$ to $E(t)$ has constant complexity. It follows that the complexity of the trajectory of $q_E(t)$ in the interval I is also $O(m)$. In turn, this implies that the function $g_q(t) = \pi(s_v(t), q_E(t))$ has only $O(m)$ breakpoints in interval I . Moreover,

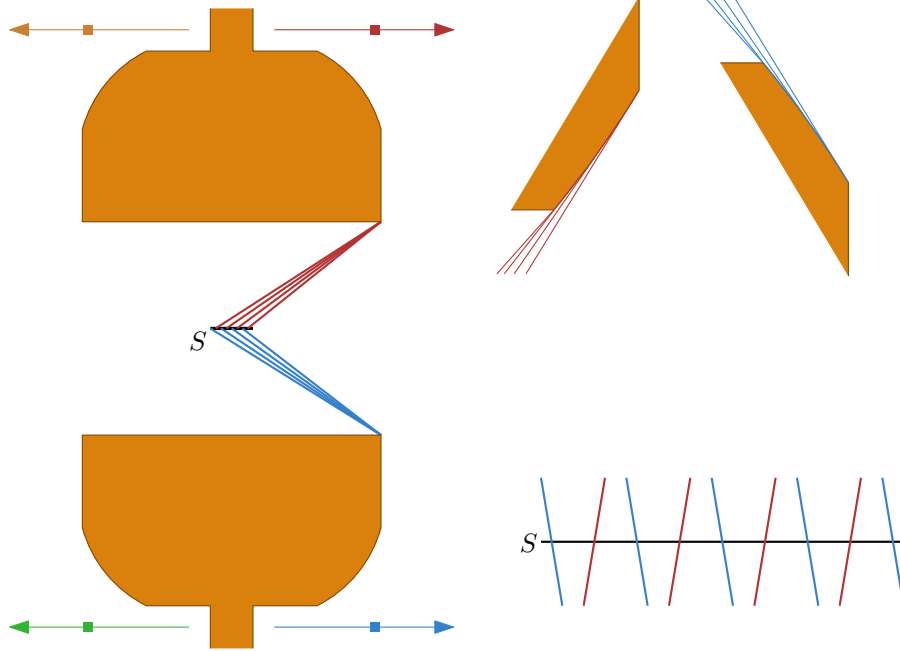


Fig. 16: An illustration of the lower bound construction for Lemma 29. The main construction is on the left, whereas the two figures on the top-right illustrated details of the right corners of the wine-glasses and the lower right is a vertically stretched depiction of the line segment S and tangents with the convex chain on the corners.

each piece of g_q is some low degree algebraic function. For $q = s_v$ and $t \in I$ we let $g_q(t)$ be undefined.

Since we have $O(mn\beta_4(n))$ intervals, it follows that the function g_q has a total complexity of $O(m^2n\beta_4(n))$.

Any 2, 3-collapse charged to v now corresponds to a vertex on the lower envelope of the functions $g_q(t)$: at such a vertex two sites, say q and r are both closest to $s_v(t)$, and there is no other site closer. The lower envelope has complexity $O(m^2n\beta_4(n)n\beta_z(n))$. It follows that there are thus also at most $O(m^2n^2\beta_4(n)\beta_z(n))$ 2, 3-collapse events charged to v . The lemma follows. \square

5.6 3,3-collapse Events

Lemma 28. *There may be $\Omega(mn^2)$ 3,3-collapse events.*

Proof. See Fig. 12(b). Again we drop points in pairs, but now the bottom of the pit contains $\Omega(n)$ sites r_1, \dots, r_h . As the bisector between p_i and q_i moves from left to right, it crosses the vertical bisector between r_j and r_{j+1} , collapsing an edge (u, v) of the Voronoi diagram. Since both u and v are degree 3 vertices, this is a 3, 3-collapse. It follows that every pair of sites p_i, q_i , generates $\Omega(mn)$ such events. The lemma follows. \square

Lemma 29. *There may be $\Omega(m^2n)$ 3,3-collapse events.*

Proof. The construction uses ideas similar to the wine-glass construction from Fig. 4. We will describe the construction in two steps as there are two different scale levels involved. The main construction is shown in Fig. 16, where we have two mirrored wine-glasses where the top of the wineglasses are right angles. If we assume the wineglasses and the four moving points are perfectly

mirrored (we will add tiny deviations later) it follows that the four points are continuously co-circular with the centerpoint moving on a horizontal line in the middle between the two wine-glasses. By tailoring the slopes of the edges along the curved parts of the wine-glasses we can ensure that the centerpoint moves left to right along a horizontal line segment $\Omega(m)$ times. We denote this line segment by S .

Next we add some variation to the two wineglasses. We replace the two right angled corners on the right with two convex chains with the following properties; (i) the lines aligned with the edges of the chain intersect the line segment S , (ii) the intersection points on S alternate between lines aligned to edges of the upper chain and of the lower chain, and (iii) when moving from left to right along S the nearest among the right two sites alternates. Note that for (iii) we will only consider the motion of the sites vertically above and below the wineglasses, so this statement does not depend on the exact location of the sites during the motion.

The bound on the number of 3,3-collapse events can then be shown from these properties. First observe that the bisector between the two left sites is still a horizontal line and the portion of it that appears in the Voronoi diagram ends in a Voronoi vertex on S . As we can make the modification to the wineglasses arbitrarily small, the main motion of the bisector between the two upper (or the two lower) vertices still remains the same. That is, it still sweeps from left to right along S . It follows that the Voronoi vertex that is the end of the bisectors of the two left vertices also sweeps from left to right on S . By property (iii) the nearest among the two right sites alternates $\Omega(m)$ times, which means that they are equidistant $\Omega(m)$ times. So with each sweep of S , there are $\Omega(m)$ points where all four sites are equidistant and it follows that there are $\Omega(m^2)$ different 3,3-collapse events.

We repeat the process with $\Omega(n)$ quadruples of points moving at significantly slower speeds. The lemma now follows. \square

Next, we prove an upper bound for the number of 3, 3-collapse events. We use the same general idea as Guibas et al. [11] use for sites moving in \mathbb{R}^2 under semi-algebraic motion. To this end, we first give some additional definitions.

Fix a pair of sites p and q . Let $m_{pq}(t)$ be the midpoint of $\pi(p(t), q(t))$. Let $B_{pq}^+(t)$ be the part of $B_{pq}(t)$ to the right/above $m_{pq}(t)$. Let $B_{pq}^+(t, \mu)$ be the point on $B_{pq}^+(t)$ at distance μ from p and q . Since geodesic μ -disks are pseudo-disks [21, 22] this function $B_{pq}^+(t, \mu)$ is well-defined (i.e. there is at most one point on $B_{pq}^+(t)$ that is at distance μ from both $p(t)$ and $q(t)$). Observe that by Theorem 15 μ_s^+ has complexity $O(m^3)$.

Lemma 30. *There are $O(m^3 n^3 \beta_z(n))$ 3, 3-collapse events.*

Proof. The bisector $B_{pq}(t)$ of p, q contains the centerpoints of geodesic disks that have p, q on their boundary. For ease of discussion let us orient the bisector and say that a point c is above a point c' on the bisector if the pseudotriangle defined by p, c, c' has those points in that clockwise order on its boundary, see Fig. 17.

Consider a centerpoint $c_{pqs}(t)$ that is on the bisector $B_{pq}(t)$ and is equidistant to $p(t), q(t)$ and $s(t)$. This centerpoint defines a geodesic disk $D_{pqs}(t)$ with radius $\mu_{pqs}(t)$ that has p, q, s on its boundary. The points p, q divide this boundary into two parts. Let $\delta D_{pqs}^+(t)$ denote the boundary section which is counterclockwise adjacent to p and $\delta D_{pqs}^-(t)$ the part that is clockwise adjacent to p . The site s can be on either boundary part. If s is on $\delta D_{pqs}^+(t)$ then for any point s' below s on the bisector, the disk centered at s' with p, q on its boundary does not contain s . Similarly any such disk for a point s'' above s does contain s .

Next let $S_{pq}^+(t)$ be the set of sites s , so that $c_{pqs}(t)$ is on $B_{pq}(t)$ (it may not be inside P for all sites s) and s is on $\delta D_{pqs}^+(t)$. Let $S_{pq}^-(t)$ be defined similarly. Then let $\min_{pq}^+(t)$ be the point of $S_{pq}^+(t)$

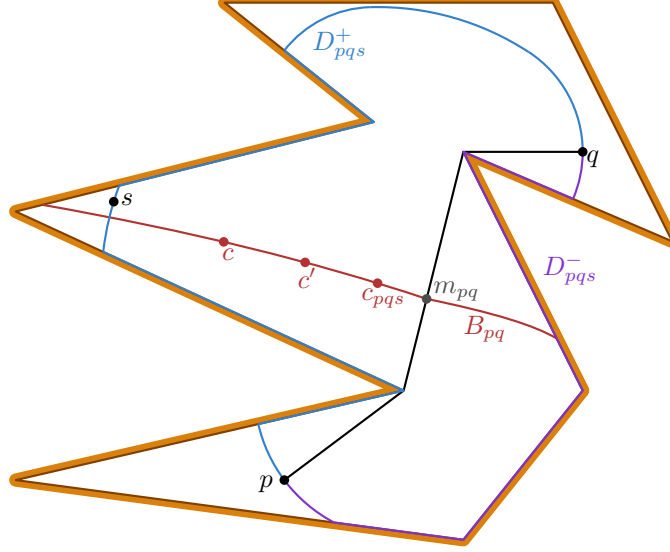


Fig. 17: An illustration of the definitions used in the proof of Lemma 30.

with the lowest centerpoint along the bisector of p, q . Also let $\max_{pq}^-(t)$ be the points of $S_{pq}^-(t)$ with the highest centerpoint along the bisector.

Now these definitions will help us count the relevant 3, 3-collapse events. For a 3, 3-collapse to occur there must be four points that are on the boundary of a geodesic disk, that is, four points are equidistant from a point inside the polygon. Furthermore, this geodesic disk must be empty of other points. Say that at a certain time t a 3, 3-event occurs between p, s, r, q with those points occurring in that clockwise order around a centerpoint c . Then following the above definitions it must be true that both s and r are in $S_{pq}^+(t)$, furthermore, since the interior of the disk must be empty, their centerpoints are the same and minimal among those in $S_{pq}^+(t)$. So for every event at a time t there must be a pair of sites p, q so that two sites s, r are both minimal among $S_{pq}^+(t)$ with respect to the bisector $B_{pq}(t)$. To count the number of events it is thus sufficient to count how often two sites can both be minimal.

To do this we would like to use some lower envelope argument. To this end, we capture the “above” and “below” measure using a function $F_{p,q}$ that maps each point on the bisector of p, q to a real value so that these real values follow the above and below definitions as larger or smaller. Let $m_{pq}(t)$ denote the midpoint of the shortest path between $p(t)$ and $q(t)$. Then for a point c on the bisector $B_{pq}(t)$ that is above $m_{pq}(t)$, we define $F_{pq}(t, c) = \pi(p(t), c) - \pi(p(t), m_{pq}(t))$. For a point c' below $m_{pq}(t)$, we define $F_{pq}(t, c') = -(\pi(p(t), c') - \pi(p(t), m_{pq}(t)))$. Then for any site $s(t)$ not equal to $p(t)$ or $q(t)$, we define $\mu_{pq}(t, s) = \perp$ (undefined) if there is no disk with a center inside P that is equidistant to p, q, s or $\mu_{pq}(t, s) = F_{pq}(t, c_{pqs})$ otherwise, where c_{pqs} is the centerpoint of the geodesic disk with p, q, s on its boundary. Finally we define $\mu_{pqs}^+(t) = \mu_{pq}(t, s)$ if $s(t) \in S_{pq}^+(t)$ and \perp otherwise. For any point s , the complexity of $\mu_{pqs}^+(t)$ is bounded by $O(m^3)$ (Theorem 15). Since we are considering $O(n)$ sites we are interested in the lower envelope of $O(n)$ functions, each consisting of $O(m^3)$ pieces of constant algebraic complexity. Therefore the number of changes in the lower envelope is bounded by $O(m^3 n \beta_z(n))$.

Counting this for every pair of sites p, q , we get a bound of $O(m^3 n^3 \beta_z(n))$ on the number of 3, 3-collapse events. \square

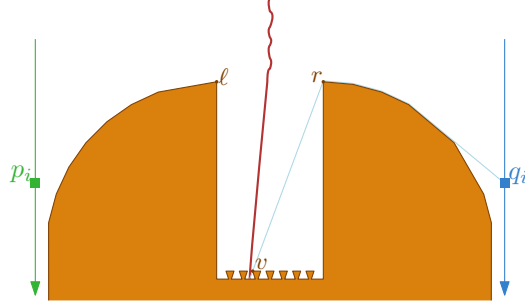


Fig. 18: An illustration of the construction that yields $\Omega(m^2n)$ 1, 2-collapse and also $\Omega(m^2n)$ vertex events.

5.7 Vertex Events

Lemma 31. *There may be $\Omega(m^2n)$ vertex events.*

Proof. We build the construction shown in Fig. 18 and we drop the sites in pairs of two, say pairs p_i, q_i . The left and right convex chains have complexity $\Omega(m)$ and are built such that the endpoint of the bisector of p_i and q_i sweeps the $\Omega(m)$ “T-shaped” obstacles every time its geodesic path to p_i or q_i changes. It now follows that the point where the bisector of p_i and q_i hits the bottom of the pit moves across the obstacles in the pit $\Omega(m)$ times. Thus the number of vertex events is $\Omega(m^2n)$. \square

Lemma 32. *The number of vertex events is at most $O(m^2n\beta_4(n))$.*

Proof. Fix a vertex v , and consider the distance from v to a site s . This distance corresponds to a piecewise hyperbolic function d_s with $O(m)$ pieces. A vertex event corresponds to a breakpoint in the lower envelope of these distance functions d_s for all sites s . Since this lower envelope has complexity $O(mn\beta_4(n))$ [25], the lemma follows. \square

5.8 A KDS for a Voronoi Diagram

In this section we develop a KDS to maintain the Voronoi diagram of S . Our KDS essentially stores for each site the extended shortest path map of its Voronoi cell, and a collection of certificates that together guarantee that the shortest paths from the sites to all Voronoi vertices remain the same (and thus the KDS correctly represents $\text{VD}_P(S)$). The main difficulties that we need to deal with are shown in Fig. 19. Here, r becomes the site closest to vertex v , and as a result a part of the polygon moves from the Voronoi cell V_p of p to the Voronoi cell V_r of r . Our KDS should therefore support transplanting this region from the SPM representation of V_p into V_r or vice versa. Moreover, part of the bisector B_{pq} becomes a bisector B_{pr} , which means that any certificates internal to the bisector (such as those needed to detect 2,2-events) change from being dependent on the movement of p to being dependent on the movement of r . Next, we show how to solve the first problem, transplanting part of the shortest path map. Our KDS for the bisector from Theorem 11 essentially solves the second problem. All that then remains is to describe how to handle each event.

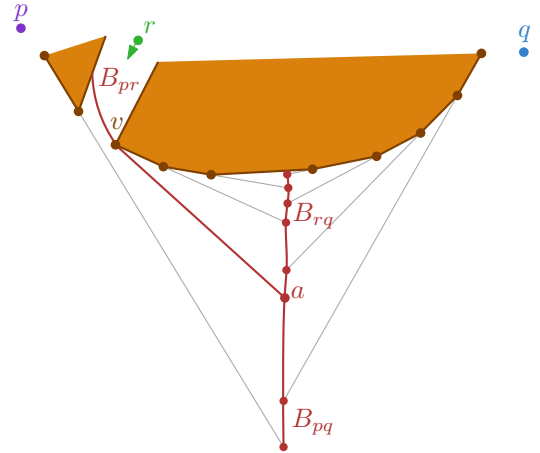


Fig. 19: A vertex event may split a bisector or a degree 3 vertex crossing an SPM extension segment may cause two bisectors to merge.

Maintaining Partial Shortest Path Maps. To support transplanting a part of SPM_s into SPM_q we extend the data structure of Aronov et al. [3]. Observe that SPM_s is a tree rooted at s , and we transplant only subtrees, rooted at some polygon vertex v . Our representation of SPM_s should support: (i) link operations in which we add the subtree rooted at v as a child of u , (ii) cut operations in which we cut an edge (u, v) , (iii) shortest path queries in which we report the length of the shortest path from some vertex u to the root s , and (iv) principal-child queries in which we report the *principal child* c of some non-root node u . The principal child is the child of u for which the angle between \overline{cu} and $\overline{up(u)}$, where $p(u)$ is the parent of u , is minimal. We need this operation to support updating the certificates of SPM_s ². To support these operations, we store SPM_s twice: once in a link-cut tree [26] and once in an Euler tour tree [12]. Both these structures support link and cut operations in $O(\log m)$ time. The link-cut trees support query operations on node-to-root paths, and hence we use them to answer shortest path queries in $O(\log m)$ time (plus $O(k)$ time to report the actual path, if desired). The Euler tour trees support query operations on subtrees, and hence we use them to answer principal child queries. In particular, we maintain the children of u in cyclic order around u , starting with c . This way link and cut operations still take $O(\log m)$ time, and the principal child of u can be reported in constant time.

The data structure. The full KDS thus consists of an extended shortest path map for every Voronoi cell maintained as described above; and certificates for each degree three vertex, degree one vertex, and each bisector. For every degree three vertex c_{pqs} we maintain the cells of SPM_p , SPM_q and SPM_s that contain it and its distance to neighboring vertices. For every degree one vertex b_{pq} , we store the cells of SPM_p and SPM_q that contain it, which edge of P it is on, and if applicable its separation from neighboring degree one vertices on the same edge. For each bisector, we store the data structure of Theorem 11. Our data structure uses a total of $O(n + m)$ space.

It is not difficult to see that this certificate structure captures all external events. For collapse and expand events involving degree three vertices we explicitly certify that the distance to its adjacent vertices is non-zero. For events involving degree one vertices we explicitly track which edge contains each such a vertex. This allows us to detect vertex events. Furthermore, we maintain distance of each degree one vertex to other degree one vertices on the same edge. Thus we can detect 1,3-expand events. Furthermore, we maintain which cells of the SPM the vertex is contained in, which allows us to detect 1,2-expand and 1,2-collapse events. What remains are the 2,2-events. These are detected by the data structure of Theorem 11.

Handling events. Handling the events is similar to what we described in Sections 3.2 and 4.2. Hence, we describe only what is new or different here.

At all external-events we have to update the shortest path map representations of the Voronoi cells. In most cases, this involves adding or removing a single vertex to the shortest path map. This can easily be handled using local computations in $O(\log^2 m)$ time. In case of vertex events, we may have to move an entire region in SPM_s to SPM_p . Since all shortest paths in such a region go via the vertex involved, we can perform these updates in $O(\log^2 m)$ time using the above data structure.

Since there are now n sites, we maintain $O(n + m)$ certificates, and thus updating the event queue takes $O(\log(n + m))$ time. Furthermore, we now have multiple degree three vertices, and thus we have to handle 3,3-collapse and expand events. These are handled in a similar fashion to the other events; we update the Voronoi regions, and compute new certificates certifying the movement of the vertices involved from scratch. All these updates can be done in $O(\log^2 m + \log n)$ time.

² Since the root is the only node storing a moving point, all certificates involve only nodes from the first three layers of the tree. Hence, it suffices to compute the principal child only for direct children of the root.

At a vertex event where p and r are equidistant to a vertex v , the region R that moves from SPM_p to SPM_r may now be bounded by a bisector B_{rq} rather than B_{pq} (see Fig. 19). Since, at the time of the event, the relevant parts of B_{pq} and B_{rq} coincide we can obtain the new part of B_{rq} by splitting B_{pq} , and updating the movement of the associated sites. In particular, replacing the function expressing the distance p to v by the distance from r to v . Our bisector KDS allows such updates in $O(\log^2 m)$ time.

Finally, we may have to update the certificates associated with the Voronoi vertices as a result of changes to the individual shortest path maps. For example, when a site s can no longer see polygon vertex v , this affects all Voronoi certificates of vertices for which the shortest path goes through v . While our KDS for the bisector (Theorem 11) can update the affected certificates of such a change efficiently, this unfortunately does not hold for the certificates associated with degree one or degree three vertices. Updating these requires $O(k(\log^2 m + \log n))$ time, where k is the number of neighbors of s in $\text{VD}_S(P)$. It is an interesting open question to try and handle such events implicitly as well. We therefore obtain the following result:

Theorem 33. *Let S be a set of n sites moving linearly inside a simple polygon P with m vertices. There is a KDS that maintains the geodesic Voronoi diagram $\text{VD}_P(S)$ that uses $O(n + m)$ space and processes at most $O(m^3 n^3 \beta_z(n))$ events, each of which can be handled in $O(k(\log^2 m + \log n))$ time, where k is the number of neighbors of the affected Voronoi cell.*

Acknowledgements. We would like to thank Man-Kwun Chiu and Yago Diez for interesting discussions during the initial stage of this research.

References

- [1] Pankaj K. Agarwal, Lars Arge, and Frank Staals. Improved dynamic geodesic nearest neighbor searching in a simple polygon. In *Proc. 34th Annual Symposium on Computational Geometry*, volume 99 of *Leibniz International Proceedings in Informatics (LIPIcs)*, pages 4:1–4:14. Schloss Dagstuhl–Leibniz-Zentrum fuer Informatik, 2018.
- [2] Pankaj K. Agarwal, Haim Kaplan, Natan Rubin, and Micha Sharir. Kinetic voronoi diagrams and delaunay triangulations under polygonal distance functions. *Discrete & Computational Geometry*, 54(4):871–904, Dec 2015.
- [3] Aronov, Guibas, Teichmann, and Zhang. Visibility queries and maintenance in simple polygons. *Discrete Comput. Geom.*, 27(4):461–483, January 2002.
- [4] Boris Aronov. On the Geodesic Voronoi Diagram of Point Sites in a Simple Polygon. *Algorithmica*, 4(1):109–140, 1989.
- [5] Boris Aronov, Steven Fortune, and Gordon Wilfong. The furthest-site geodesic voronoi diagram. *Discrete & Computational Geometry*, 9(3):217–255, Mar 1993.
- [6] Julien Basch, Leonidas J. Guibas, and John Hershberger. Data structures for mobile data. *J. Algorithms*, 31(1):1–28, 1999.
- [7] G. S. Brodal and R. Jacob. Dynamic planar convex hull. In *The 43rd Annual IEEE Symposium on Foundations of Computer Science, 2002. Proceedings.*, pages 617–626, Nov 2002.
- [8] Erik D. Demaine, Joseph S. B. Mitchell, and Joseph O’Rourke. The open problems project. <http://maven.smith.edu/~orourke/TOPP/>.

- [9] J. E. Goodman and J. O'Rourke. *Handbook of Discrete and Computational Geometry*. CRC Press series on discrete mathematics and its applications. Chapman & Hall/CRC, 2004.
- [10] Leonidas Guibas, John Hershberger, Daniel Leven, Micha Sharir, and Robert E. Tarjan. Linear-time algorithms for visibility and shortest path problems inside triangulated simple polygons. *Algorithmica*, 2(1):209–233, Nov 1987.
- [11] Leonidas J. Guibas, Joseph S. B. Mitchell, and Thomas Roos. Voronoi diagrams of moving points in the plane. In *Graph-Theoretic Concepts in Computer Science*, pages 113–125, Berlin, Heidelberg, 1992. Springer.
- [12] Monika R. Henzinger, Valerie King, and Valerie King. Randomized fully dynamic graph algorithms with polylogarithmic time per operation. *J. ACM*, 46(4):502–516, July 1999.
- [13] John Hershberger and Subhash Suri. An Optimal Algorithm for Euclidean Shortest Paths in the Plane. *SIAM Journal on Computing*, 28(6):2215–2256, 1999.
- [14] Menelaos I. Karavelas and Leonidas J. Guibas. Static and kinetic geometric spanners with applications. In *Proceedings of the Twelfth Annual ACM-SIAM Symposium on Discrete Algorithms*, SODA '01, pages 168–176, Philadelphia, PA, USA, 2001. Society for Industrial and Applied Mathematics.
- [15] Chih-Hung Liu. A Nearly Optimal Algorithm for the Geodesic Voronoi Diagram of Points in a Simple Polygon. In *34th International Symposium on Computational Geometry (SoCG 2018)*, volume 99 of *Leibniz International Proceedings in Informatics (LIPIcs)*, pages 58:1–58:14, Dagstuhl, Germany, 2018. Schloss Dagstuhl–Leibniz-Zentrum fuer Informatik.
- [16] Anna Lubiw, Jack Snoeyink, and Hamideh Vosoughpour. Visibility graphs, dismantlability, and the cops and robbers game. *Computational Geometry*, 66:14 – 27, 2017.
- [17] J. S. B. Mitchell. Shortest paths among obstacles in the plane. In *Proc. 9th Annu. ACM Sympos. Comput. Geom.*, pages 308–317, 1993.
- [18] Joseph S. B. Mitchell. A new algorithm for shortest paths among obstacles in the plane. *Annals of Mathematics and Artificial Intelligence*, 3(1):83–105, Mar 1991.
- [19] Eunjin Oh. Optimal algorithm for geodesic nearest-point voronoi diagrams in simple polygons. In *Proceedings of the Thirtieth Annual ACM-SIAM Symposium on Discrete Algorithms*, pages 391–409. SIAM, 2019.
- [20] Eunjin Oh and Hee-Kap Ahn. Voronoi diagrams for a moderate-sized point-set in a simple polygon. *Discrete & Computational Geometry*, Mar 2019.
- [21] Eunjin Oh, Sang Won Bae, and Hee-Kap Ahn. Computing a geodesic two-center of points in a simple polygon. *Computational Geometry*, 82:45 – 59, 2019.
- [22] Eunjin Oh, Jean-Lou De Carufel, and Hee-Kap Ahn. The 2-center problem in a simple polygon. In *Algorithms and Computation*, pages 307–317, Berlin, Heidelberg, 2015. Springer Berlin Heidelberg.
- [23] Evanthia Papadopoulou and Der-Tsai Lee. A New Approach for the Geodesic Voronoi Diagram of Points in a Simple Polygon and Other Restricted Polygonal Domains. *Algorithmica*, 20(4):319–352, 1998.

- [24] Natan Rubin. On kinetic delaunay triangulations: A near-quadratic bound for unit speed motions. *J. ACM*, 62(3):25:1–25:85, June 2015.
- [25] Micha Sharir and Pankaj K Agarwal. *Davenport-Schinzel sequences and their geometric applications*. Cambridge university press, 1995.
- [26] Daniel D. Sleator and Robert Endre Tarjan. A data structure for dynamic trees. *Journal of Computer and System Sciences*, 26(3):362 – 391, 1983.
- [27] Subhash Suri. A linear time algorithm with minimum link paths inside a simple polygon. *Computer Vision, Graphics and Image Processing*, 35(1):99–110, 1986.